UDC 541.6:541.49:546.77

HETEROBIMETALLIC DIOXOMOLYBDENUM(VI) COMPLEXES DERIVED FROM BIS(2-HYDROXY-1-NAPHTHALDEHYDE)MALONOYLDIHYDRAZONE: SYNTHESIS AND CHARACTERIZATION

A. Kumar[1], O.B. Chanu[2], A. Koch[2], R.A. Lal[2]

[1]*Department of Chemistry, The University of the West Indies, St. Augustine, Trinidad and Tobago, West Indies*
 E-mail: Arvind.Kumar@sta.uwi.edu
[2]*Department of Chemistry, North Eastern Hill University, Meghalaya, India*

The heterobimetallic complexes $[MMoO_2(L)(H_2O)_2]$ (where $M = Zn^{2+}$ (**1**), Cu^{2+} (**2**), and Co^{2+} (**4**)) and $[\{MMoO_3(H_2L)(H_2O)_2\}_2]$ (where $M = Ni^{2+}$ (**3**) and Mn^{2+} (**5**)) are synthesized from bis(2-hydroxy-1-naphthaldehyde)malonoyldihydrazone (H_4L) using the monometallic precursor complex $[MoO_2(H_2L)] \cdot H_2O$ in ethanol. The composition of the complexes is established based on the data obtained from the elemental analysis and molecular weight determinations. The structure of the complexes is discussed in the light of data obtained from molar conductance, magnetic moment, electronic, EPR and IR spectroscopic studies.

K e y w o r d s: bis(2-hydroxy-1-naphthaldehyde)malonoyldihydrazone, heterobimetallic, dioxomolybdenum, dioxouranium, magnetic moment, spectroscopic studies.

INTRODUCTION

Molybdenum occurs in nature in combination with copper in the unique heterobimetallic enzyme carbon monoxide dehydrogenase [1]. This enzyme catalyzes the oxidation of CO to CO_2, thereby providing both carbon source and energy to the organism for growth and maintaining a sub-toxic level of CO in the atmosphere. The molybdenum ion shows an antagonistic function with regard to copper in humans and animals [2]. Molybdenum-copper complexes or tungsten-copper complexes combining polyfunctional ligands constitute an interesting system for research due to their diverse structural chemistry and relevance to biological systems [3]. Molybdenum is present in the heterobimetallic enzyme nitrogenase along with iron which is present in free living and symbiotic microorganisms catalyses the reduction of atmospheric dinitrogen to ammonia [4]. The chemistry of molybdenum attracts attention not only in view of its role in the biosphere as an essential element, but also due to importance in catalysis [6—8]. In catalysis, a heterobimetallic complex containing an electron deficient metal atom and an electron rich metal atom presents the possibility of Lewis acid activation of a substrate molecule bound to the electron rich metal centre due to the electronic interaction between metals and cooperative activation of the substrate [9, 10]. These complexes might be helpful in investigating the mutual influence of the two metal centres on the electronic, magnetic, and redox properties of such systems [11, 12]. A cobalt or nickel promoted molybdenum catalyst is important in industrial catalysis, particularly in the hydrosulfurization process [13, 14] whereby organosulfur compounds in petroleum feed stocks are heterogeneously desulfurized with dihydrogen.

The dihydrazone ligand is a multifunctional ligand with as many as eight bonding sites, naphtholic —OH, azomethine, secondary —NH, and carbonyl oxygen in duplicate in its molecular skeleton capable of giving rise to mononuclear and polynuclear homo- and heterometal complexes [15, 16].
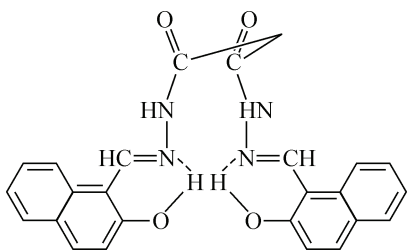
Fig. 1. Structure of bis(2-hydroxy-1-naphthaldehyde)malonoyldihydrazone (H_4L) ligands

A survey of the literature reveals that although works on metal complexes of monohydrazide based ligands and their Schiff bases have been carried out in some details [17—19], but those on metal complexes of dihydrazones containing active methylene functions are quite meagre. It further reveals that the work on heterobimetallic complexes of such dihydrazones is virtually absent. In view of the above importance of the heterobimetallic complexes of molybdenum and the virtual absence of work on heterometallic complexes of dihydrazones, the present paper aims to describe the synthesis of some heterobimetallic complexes of molybdenum in its 6+ oxidation state, derived from the polyfunctional dihydrazone (H_4L) ligand (Fig. 1). Accordingly, the paper describes the synthesis of heterobimetallic complexes of molybdenum and some first row transition metal ions derived from the title ligand. The complexes were mainly characterized based on the elemental analyses and molecular weight determinations. The structure of the complexes has been discussed in the light of molar conductivity, ^1H NMR, IR spectra, magnetic moment, EPR, and electronic spectral data.

EXPERIMENTAL

Ammonium molybdate $(NH_4)_6Mo_6O_{24} \cdot 4H_2O$, metal acetates, ethyl malonate, hydrazine hydrate, 2-hydroxy-1-naphthaldehyde, acetylacetone were of Aldrich or equivalent grade. Malonoyldihydrazine (MDH), H_4L ligand, and $MoO_2(acac)$ were prepared by the literature methods [15, 20]. The monometallic dioxomolybdenum complex $[MoO_2(H_2L)] \cdot H_2O$ was prepared by the reaction of molybdenyl acetylacetone with the H_4L ligand in the 1:1 molar ratio in ethanol [15]. The determination of molybdenum and other transition metal ions was performed following the standard literature procedures [21]. The magnetic susceptibility measurements were carried out on a Model 155 BAR vibrating sample magnetometer fitted with a Walker Scientific L75BAL magnet. The molar conductance of the complexes was measured on a Direct Reading Conductivity meter-303 with a dip type conductivity cell at room temperature in DMSO (10^{-3} M). Molecular weights were determined in a DMSO solution by the freezing point depression method. Infrared spectra were recorded on a Paragon 500-model infrared spectrophotometer in the range 4000—350 cm^{-1} in KBr discs. ^1H NMR spectra of dihydrazone and metal complexes were recorded on an EM-390, 90 MHz spectrophotometer in DMSO-d_6. The electronic spectra of the complexes were recorded on a Milton Roy Spectronic-21 spectrometer. The EPR spectra of the complexes were recorded at an X-band frequency on a Varian E-112 E X1Q-band spectrometer using DPPH ($g = 2.0036$) as an internal field marker.

Preparation of the complexes $[MMoO_2(L)(H_2O)_2]$ (where $M = Zn^{2+}$ (1), Cu^{2+} (2), Co^{2+} (4)) and $[\{MMoO_3(H_2L)(H_2O)_2\}_2]$ (where $M = Ni^{2+}$ (3), Mn^{2+} (5)). In order to prepare the $[ZnMoO_2(L)(H_2O)_2]$ complex (**1**), the $[MoO_2(H_2L)] \cdot H_2O$ complex (0.584 g, 1.0 mmol) was taken in ethanol (50 ml) and stirred gently over a period of 10—15 min to make the suspension homogeneous. This was added to a solution of $Cu(OAc)_2 \cdot 2H_2O$ (1.20 mmol) in ethanol (50 ml), maintaining the molar ratio at 1:1.2. The reaction mixture was further stirred for about 30 min, and refluxed for 3 h, which produced a yellow precipitate. The precipitate was filtered, washed with ethanol, ether and dried under vacuo over anhydrous $CaCl_2$. Yield: 0.59 g (60 %).

Complexes (**2**) to (**5**) were also prepared by adopting the procedure given above and using the respective metal acetates (M = Cu(II), Ni(II), Co(II), Mn(II)) instead of copper (II) acetate. Yield: (60—65) %.

RESULTS AND DISCUSSION

The heterobimetallic complexes of $MoO_2(VI)$ were synthesized by adopting the strategies developed by Lintvedt *et al.* [22] and Davies *et al.* [23]. The monometallic dioxomolybdenum (VI) complex $[MoO_2(H_2L)] \cdot H_2O$ was allowed to react with $Zn(OAc)_2 \cdot 2H_2O$ or other metal acetates (M =

Complex, color, analytical, molar conductance, magnetic moment and electronic spectral data for heterobimetallic dioxomolybdenum(VI) complexes

Sl. No.	Complex (Color)	Yield, %	Mol. Wt. (calcd.)	Elemental analyses: Found (calcd.), %					Molar cond., Λ_M, $ohm^{-1} \cdot cm^2 \cdot mol^{-1}$	Magnetic moment μ_{eff} B.M.	Electronic spectral band λ_{max}, nm (ϵ_{max}, $dm^3 \cdot mol^{-1} \cdot cm^{-1}$)
				Mo	M	C	H	N			
	H$_4$L	—	—	—	—	68.45 (68.18)	4.62 (4.55)	13.00 (12.73)	—	—	320 (9500), 390 (15700), 340 (11225)
1	[ZnMoO$_2$(L)(H$_2$O)$_2$] (Yellow)	65	750±35 (665.38)	14.03 (14.43)	9.43 (9.83)	40.60 (40.09)	2.98 (3.01)	8.11 (8.42)	7.0	—	400 (12980), 430 (9890), 475 (5760)
2	[CuMoO$_2$(L)(H$_2$O)$_2$] (Brown)	64	770±40 (663.55)	15.02 (14.47)	9.15 (9.58)	45.91 (45.21)	2.95 (3.01)	8.82 (8.44)	5.3	2.05	335 (9870), 420 (12750), 740 (210), 830 (250)
3	[NiMoO$_3$(H$_2$L)(H$_2$O)$_2$]$_2$ (Greenish-yellow)	62	1520±60 (1353.38)	13.75 (14.19)	8.25 (8.68)	45.10 (44.33)	3.19 (3.25)	8.05 (8.28)	3.8	2.94	405 (12570), 620 (45), 960 (37)
4	[CoMoO$_2$(L)(H$_2$O)$_2$] (Yellow)	63	750±40 (658.93)	14.11 (14.57)	8.79 (8.94)	46.13 (45.53)	3.09 (3.04)	8.35 (8.50)	2.5	4.53	400 (10580), 460 (5760), 530 (810), 630 (630), 640 (545)
5	[MnMoO$_3$(H$_2$L)(H$_2$O)$_2$]$_2$ (Orangish-yellow)	60	1550±70 (1345.88)	13.97 (14.27)	8.55 (8.17)	45.20 (49.08)	3.22 (3.27)	8.61 (8.32)	3.0	6.48	400 (12570), 510 (6740)

= Cu(II), Ni(II), Co(II), Mn(II)) in a 1:1.2 molar ratio in absolute ethanol under reflux. All the complexes with their color, analytical, magnetic moment, molar conductance and absorption data are given in the Table 1. These complexes are air-stable and decompose above 300 °C. The complexes are insoluble in water and common organic solvents such as ethanol, methanol, ether, chloroform, dichloromethane, acetone, etc. but are soluble in DMSO and DMF. The molar conductance value of the complexes in a DMSO solution at a 10^{-3} M concentration falls in the range 2.5—7.0 Ohm^{-1} cm^2 mol^{-1}, suggesting that they are non-electrolyte in this solvent [24]. All of the complexes were heated at 110 °C and 180 °C and the weight loss was determined. None of the complexes showed weight loss at 110 °C, ruling out the possibility of the presence of water molecules in their lattice structure. On the other hand, the complexes showed weight loss corresponding to two water molecules at 180 °C suggesting that they are coordinated to the metal centre [25]. The vapour evolved at 180 °C was passed through a trap containing anhydrous CuSO$_4$ which turned blue indicating that it originates from water molecules.

Molecular weight. The molecular weight data for the complexes (Table 1) have been determined in spectral grade DMSO by the freezing point depression method. The experimental values of molecular weights for complexes (**1**), (**2**), and (**4**) are very close to the values calculated based on their monomer formulation confirms the monomeric character. On the other hand, the experimental values of the molecular weights for complexes (**3**) and (**5**) agree with their dimeric character. However, the

experimental values of the molecular weights are slightly higher than those calculated on the basis of the suggested monomer or dimer formulation. Such higher values of the molecular weights strongly suggest that the structure of the complexes is altered in the strong coordinating solvent as compared to that in the solid state. Most probably, the coordinated water molecules are substituted by DMSO molecules, which accounts for the higher molecular weights of the complexes.

Magnetic moment. The observed zero magnetic moment values of complex (**1**) indicates its diamagnetic character. The diamagnetic character of this complex is consistent with the d^{10}, d^0, and f^0 configuration of zinc and molybdenum in this complex indicating their presence in +2 and +6 oxidation states respectively. The μ_{eff} magnetic moment values for heterobimetallic Cu—MoO$_2$ complex (**3**) is 2.05 B.M., which rules out the possibility of any appreciable spin-spin coupling between the unpaired electrons belonging to copper. The μ_{eff} value of the complex suggests that the copper(II) centre has a pseudotetrahedral geometry as supported by the electronic and ESR spectral studies discussed below. The observed magnetic moment values of heterobimetallic Ni—MoO$_3$ (**3**) and Mn—MoO$_3$ (**5**) complexes are 2.94 B.M. and 6.08 B.M., respectively. These values are characteristic of octahedral Ni(II) and high-spin octahedral Mn(II) complexes. The magnetic moment value of heterobimetallic Co—MoO$_2$ complex (**4**) is 4.53 B.M. The magnetic moment values for octahedral and tetrahedral cobalt(II) complexes lie in the rage of 4.70—5.60 B.M. and 4.20—4.80 B.M., respectively [27]. Thus, the observed μ_{eff} value of 4.53 B.M. corresponds to the tetrahedral complex, which is consistent with the occurrence of a very strong absorption band around 610 nm with a multiple-structure in the electronic spectrum of the complex. The μ_{eff} value for the complex also rules out the possibility of any metal-metal interaction in the structural unit of the complex.

Electronic spectra. The electronic spectral bands together with molar extinction coefficients for the complexes have been set out in Table 1. The free H$_4$L ligand shows two bands at 320 nm (ε_{max}, 9500 dm$^3 \cdot$mol$^{-1} \cdot$cm^{-1}) and 390 nm (ε_{max}, 15700 dm$^3 \cdot$mol$^{-1} \cdot$cm^{-1}) in the region 300—400 nm. The band at 320 nm is assigned as an intra-ligand $\pi \rightarrow \pi^*$ transition, while the band at 390 nm is assigned to an $n \rightarrow \pi^*$ transition. The band at 390 nm is characteristic of the naphthaldimine part of the ligand, as has been reported for several monoacylhydrazones [15, 28, 29]. The electronic spectra of the complexes also show two bands in the region 300—450 nm, which is indicative of their discrete molecularity [20, 25]. The ligand bands at 320 nm and 390 nm showed a red shift on complexation to metal. The band appearing in the region 340—390 nm is attributed to a $\pi \rightarrow \pi^*$ transition corresponding to the ligand band at 320 nm. On the other hand, the band appearing in the region 410—430 nm may be assigned to arise due to the ligand band at 390 nm and could be attributed to the $n \rightarrow \pi^*$ transition. The red shift of ligand bands by 20—70 nm and 20—40 nm gives good evidence of chelation of dihydrazone to the metal centre. The magnitude of the shift of ligand bands on complexation indicates strong bonding between the ligand and the metal centre. Heterobimetallic Zn—MoO$_2$ complex (**1**) also shows a weak band at 475 nm ($\varepsilon = 5740$ dm$^3 \cdot$mol$^{-1} \cdot$cm^{-1}) which is assigned to be originating from the ligand-to-metal charge transfer [31]. Heterobimetallic Cu—MoO$_2$ complex (**2**) shows two bands at 740 nm and 830 nm, which are assigned to the ligand field transition. The position of these bands is consistent with distorted tetrahedral stereochemistry of copper(II) complexes tending towards planarity [32, 33]. Heterobimetallic Ni—MoO$_3$ complex (**3**) shows two bands at 960 nm and 620 nm in the region 500—1000 nm, which indicates that the complex has distorted octahedral stereochemistry. A comparison of the position of the absorption bands in the spectrum of complex (**4**) with that of [Ni(H$_2$O)$_6$]$^{2+}$ at 1175 nm and 749 nm and that of [Ni(NH$_3$)$_6$]$^{2+}$ at 935 nm and 570 nm suggests that the first band bears similarity with nitrogen donor ligands, while the second band has the position close to the average position of the corresponding band in the oxygen donor ligands and nitrogen donor ligands [34]. This, in turn, suggests that the nickel atom occupies the N$_2$O$_2$ coordination sphere, *i.e.*, it has displaced molybdenum from the N$_2$O$_2$ coordination sphere. The various ligand field parameters listed in the table below for this complex have been calculated using the equations given by Lever [35].

Complex	$^3A_2 \to {}^3T_{2g}(F)$ ν_1, cm^{-1}	$^3A_2 \to {}^3T_{2g}(F)$ ν_2, cm^{-1}	B	β	β^0	ν_2/ν_1	LFSE, kcal/mol
[NiMoO$_3$(CH$_2$LH$_2$)(H$_2$O)$_2$]	10416	16130	683	0.631	36.9	1.55	9.67

Heterobimetallic Co—MoO$_2$ complex (**4**) shows a multiple-structured band at ca. 610 nm with absorption bands in the region 640—580 nm (ε = 810–545 dm$^3\cdot$mol$^{-1}\cdot$cm^{-1}). The tetrahedral cobalt(II) complexes show three absorption bands corresponding to the transitions $^4A_2 \to {}^4T_2$(F) (2000—3300 nm, ν_1), $^4A_2 \to {}^4T_1$(F) (1250—2500 nm, ν_2) and $^4A_2 \to {}^4T_1$(P) (500—650 nm, ν_3) [36]. The first band ν_1, owing to its position in the spectrum has been obscured and is orbitally forbidden as well. However, the second band corresponding to the ν_2 transition is usually broad and appears in the near infrared region, and the third transition ν_3 is intense, broad and usually exhibits a great deal of structure [37]. The extinction coefficient of the absorption band in complex (**4**) is much higher as compared to those generally observed for octahedral cobalt complexes, therefore, it is suggested that the cobalt (II) centre has a tetrahedral geometry in this complex. Heterobimetallic Mn—MoO$_3$ complex (**5**) shows only one band at 400 nm and a non-ligand band at 510 nm. The very high molar extinction coefficient for this band indicates that it has a charge-transfer character. The d—d transition occurring in this region due to the Mn(II) centre in this complex is masked by a strong charge-transfer band.

Electron paramagnetic resonance (EPR). The various EPR parameters for complexes (**2**), (**3**) and (**5**) have been set out in Table 2. The EPR spectrum of complex (**2**) is shown in Fig. 2. The magnetic moment value for heterobimetallic Cu—MoO$_2$ complex (**2**) suggests that the complex has a discrete molecularity. The complex at RT in the solid state shows the isotropic spectrum with the g_{av} value of 2.102. The ESR spectrum of the complex is rhombically distorted at LNT in CH$_3$CN-DMSO glass and the spectral feature of the complex can be explained by assuming C_{2v} symmetry [38]. In this symmetry three possible mechanisms can split g_x and g_y, which are:

i)   differences in E_{xz} and E_{yz} values;
ii) differences in reduction factors (excited state delocalization); and
iii) magnitude of dz^2 mixing into the ground state wave functions.

T a b l e   2

EPR parameters for Cu—MoO$_2$ (3), Ni—MoO$_3$ (4) *and* Mn—MoO$_2$ (6) *heterobimetallic complexes*

Complexes	Temp (state)	g_{av}	$g_1/g_\parallel$	g_2	$g_3/g_\perp$	A_{av}	$A_1/A_\parallel$ (G)	A_2 (G)	$A_3/A_\perp$ (G)
[CuMoO$_2$(L)(H$_2$O)$_2$] (**2**)	RT (Solid)	2.102	—	—	—	—	—	—	—
	LNT (CH$_3$CN-DMSO)	2.102	2.358(g_z)	2.047(g_y)	2.000 (g_x)	72	180(A_z)	18(A_y)	—
[NiMoO$_3$(H$_2$L)(H$_2$O)$_2$] (**3**)	RT (Solid)	2.005	—	—	—	—	—	—	—
	LNT (CH$_3$CN-DMSO)	2.005	—	—	—	—	—	—	—
[MnMoO$_3$(H$_2$L)(H$_2$O)$_2$] (**5**)	RT (Solid)	1.988	—	—	—	—	—	—	—
	LNT (CH$_3$CN-DMSO)	2.021	—	—	—	94	—	—	—

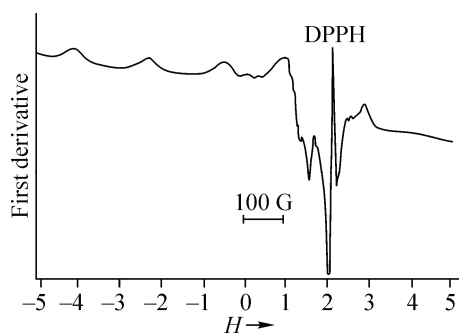*Fig. 2.* EPR spectrum of $[CuMoO_2(L)(H_2O)_2]$ complex (**2**) at 293 K in the solid state

It has been reported that for a difference of about 125 nm between E_{xz} and E_{yz} values, the difference $(g_x - g_y)$ can be as much as 0.004 [38]. In the present case, two ligand field transitions have been observed, which differ by ~90 nm while the difference between g_x and g_y is 0.047. Therefore, the above point (i) cannot account for such a large splitting in g-parameters. The major contributing factor(s) towards the rhombic splitting for the complex should be either due to dz^2 mixing into the ground state wave function or extensive excited state delocalisation or both.

In probing the ESR spectral characteristics of plastocyanin, a copper containing protein, it has been argued in favour of an anisotropic declocalization over the cysteine sulfur p_π-orbital [39]. However, the extent of g-splitting in plastocyanin cannot be explained by considering orbital reduction factors alone due to their small effects. On the other hand, this splitting is quite sensitive to the amount of dz^2 mixing into the ground state wave function. A mixing of about 3 % of the dz^2 orbital into the ground state could satisfactorily explain the observed g-splitting in the case of stellocyanin. The difference between A_x and A_y values could also be explained with this amount of mixing of the dz^2 orbital into the ground state. Belford *et al.* [40] defined a parameter R_g in order to evaluate the extent of dz^2 orbital mixing into the ground state by ignoring the orbital reduction factor.

$$R_g = (g_x - g_y)/\{0.5(g_x + g_y) - 2.0023\}.$$

R_g is thus a measure of the degree of rhombic splitting in the g-values, which is a steep function of the extent of dz^2 mixing. The R_g value for this complex is 2.2, therefore, a mixing of the order of 6.0—7.5 % can satisfactorily account for the g-split observed. For 4—5 % mixing, the difference $A_x - A_y$, should be about 60×10^{-4} cm^{-1}. However, the difference $A_x - A_y$ could not be calculated in the present case since the spectrum did not show a metal-hyperfine splitting in the g_x region.

The EPR spectrum of complex (**3**) at 9.1 GHz shows a single signal at $g = 2.005$ in the polycrystalline form both at RT and LNT. This signal is attributed to arise from the double quantum transition [41]. In the Ni (II) complex, the zero-field splitting (ZFS) ranges from a few to some tens of the wave number [42—44]. Consequently the conventional X-band and g-band EPR spectroscopy arsing electromagnetic quanta around 0.3 cm^{-1} and 1.5 cm^{-1} respectively find it difficult to excite transitions between the states of the spin-triplet manifold [44]. The square planar complexes are EPR silent while four-coordinated tetrahedral and six coordinate octahedral complexes are EPR active. The complex shows an intense signal with $g = 2.005$, which suggests that nickel has either an octahedral or tetrahedral geometry. Further, the g-value for nickel complexes depends on the donor set as well as on the coordination geometry of the complex. Nickel(II) complexes with oxygen donors (donor set NiO_6) have a g-value greater than 2.2, whereas those with nitrogen donors (donor NiN_6) generally have a g-value either of 2.2 or less. The value $g = 2.005$ in complex (**3**) is less than 2.2, as is expected for the NiN_2O_4 donor set [42, 45]. The intensity of the signal at $g = 2.005$ remains unchanged at RT as compared to LNT, ruling out the possibility of impurity [46].

Heterobimetallic Mn—MoO$_3$ complex (**5**) shows an isotropic signal at RT in the solid state with $g \cong 2.0$, while in a CH$_3$CN-DMSO solution at LNT it shows a six-line spectrum with a ^{55}Mn hyperfine splitting of 94 G. This hyperfine splitting constant is characteristic of Mn(II) complexes rather than of Mn(IV) complexes [47]. At LNT between every pair of the six hyperfine lines at $g \cong 2.0$ resonance, there is a pair of relatively weak forbidden transitions.

^{1}H NMR spectra. Heterobimetallic complex (**1**) has been characterized by ^{1}HNMR spectroscopy as well. However, the ^{13}C NMR spectra of the complexes in DMSO-d_6 were featureless due to their poor solubility. Hence, these complexes could not be characterized by ^{13}C NMR spectroscopy. The ^{1}H NMR spectral data for free dihydrazone, the precursor monometallic [MoO$_2$(H$_2$L)]·H$_2$O complex, and the heterobimetallic complexes and the assignment of the signals are given in Table 3.

T a b l e 3

¹HNMR *spectral data* (*in* ppm) *for heterobimetallic complexes containing dioxouranium*(VI),
dioxomolybdenum(VI) *and zinc*(II)

Complex	δ(—CH$_2$—)	δ(naphthyl)	δ(—CH=N—) (J, Hz)	δ(OH)+δ(NH) (J, Hz)
LH$_4$	3.90	8.30—7.03 (m)	9.31 (d, 32.9)	12.65 (d, 63.0)
	3.60		9.60 (d, 32.9)	11.50 (d, 63.0)
[MoO$_2$(H$_2$L)]·H$_2$O	3.58	8.72—7.15 (m)	9.80 (d, 45.0)	12.56 (d, 45.0)
			8.96 (d, 45.0)	11.49 (d, 45.0)
[ZnMoO$_2$(L)(H$_2$O)$_2$] (**1**)	3.63	8.57—7.05 (m)	9.72 (d, 34.2)	—
			8.84 (d, 34.2)	

The ¹H NMR spectrum of the heterobimetallic complex (**1**) shows different features as compared to those of free dihydrazone and the precursor monometallic molybdenum complex. The doublets observed at δ 12.65 ppm and 11.50 ppm in uncoordinated dihydrazone and at δ 12.46 ppm and 11.49 ppm in the precursor monometallic complex disappear on the heterobimetallic complex formation. This indicates the collapse of the amide structure of the ligand in the heterobimetallic complexes. The signals corresponding to azomethine protons appear as doublets similar to those in uncoordinated dihydrazone and the precursor monometallic complex. The δ-CH=N— signals are shifted upfield by 0.18 ppm and 0.11 ppm as compared to those in the precursor complex. However, these signals are still shifted downfield by 0.24 ppm and 0.32 ppm as compared to those in uncoordinated dihydrazone. Such features associated with the shifts of δ-CH=N— proton signals may arise due to the flow of the electron density of the second metal centre through enolate oxygen atoms, suggesting the bonding through *enolate* oxygen atoms to the second metal centre. This, in turn, may reduce the amount of charge flowing to the original metal centre through the azomethine nitrogen atom, indicating that the metal-nitrogen bond is weaker in these complexes than that in the precursor monometallic molybdenum complex [48, 49]. The appearance of δ-CH=N— proton resonances in the form of doublets confirms that dihydrazone is coordinated to the metal centres in the *anti-cis* configuration just as in the precursor monometallic complex [49].

Infrared spectra. Structurally significant IR spectral bands for H$_4$L, the precursor monometallic dioxomolybdenum complex, and heterobimetallic MoO$_2$ complexes are summarized in Table 4. A comparison of the IR spectra of the heterobimetallic complexes with those of the ligand and the precursor complex suggests that dihydrazone is present in the *enol* form in heterobimetallic complexes (**1**), (**2**), and (**4**), whereas it is present in the *keto* form in heterobimetallic complexes (**3**) and (**5**) [49]. The present ligand shows strong broad bands centred at 3450 cm^{-1}, 3200 cm^{-1}, and 3047 cm^{-1}. These bands are assigned to arise from the stretching vibrations of naphtholic OH and secondary NH groups respectively [30]. Complexes (**5**) and (**6**) show a strong broad band in the range 3550—3000 cm^{-1} with peaks in 3420—3400 cm^{-1} and 3220—3186 cm^{-1} regions respectively. On the other hand, the remaining complexes show only a single strong broad band in the 3550—3000 cm^{-1} region with a peak in the 3420—3400 cm^{-1} region. In all the complexes, the essential feature of the peak in the 3420—3400 cm^{-1} region resembles in shape and position those commonly observed for water or ethanol and has been, accordingly, assigned to the ν(OH) mode. From the position and intensity of the ν(OH) mode of water and ethanol it is not possible to distinguish whether they are coordinated to the metal centre or present as uncoordinated in the lattice. However, the presence of a band in the 670—644 cm^{-1} region in the complexes assigned to the ρ_r mode of coordinated water suggests unambiguously that these are water molecules present in the first coordination sphere around the metal centre in the complexes, rather than the ethanol molecules [50]. All complexes show a weight loss at 180 °C corresponding to two water molecules, lending credence to the suggested number of coordinated water molecules in the complexes. The fact that the weight loss occurs due to the water molecules only was confirmed by passing the ensuing vapour through a trap containing anhydrous copper sulphate that

T a b l e 4

Infrared spectral data for heterobimetallic dioxomolybdenum (VI) *complexes*

Sl. No	Ligand/complex	ν(OH)+ν(NH)	Amide I ν(C=O)	ν(>C=N—N=C<)	Amide II + ν(C—O) (phenolic)	ν(NCO)	β(C—O)	ν(N—N)	ν(MoO$_2^{2+}$)	ν(M—O) (naphtho)	ν(—O) (carbonyl)
	H$_4$L	3450sbr 3200s 3047s	1699vs 1661vs	1617vs 1596vs	1532vs	—	1278s	1030w	—	—	—
	[MoO$_2$(H$_2$L)]·H$_2$O	3368s 3184s	1669 s	1616 s 1595 s	1551 s 1538s	—	1280m	1033 w	938vs 910vs	591s	
1	[ZnMoO$_2$(L)(H$_2$O)$_2$]	3500—3300 sbr	—	1615vs 1599vs	1534vs	—	1277m	1095w	941s 907s	591w 530w	455w
2	[CuMoO$_2$(L)(H$_2$O)$_2$]	3500—3000 sbr	—	1615vs 1599vs	1530vs	—	1277w	1066m	939vs 913vs	593w 530w	454w
3	[NiMoO$_3$(H$_2$L)(H$_2$O)$_2$]$_2$	3400 vs 3140vs	1693vs 1666vs	1617vs 1598vs	1531s	—	1280m	1037w	939vs 909vs 875vs	554m 527m	—
4	[CoMoO$_2$(L)(H$_2$O)$_2$]	3420sbr 3035s	—	1616s 1600s	1536vs	—	1287w	1037w	941s 904s	593m	484m
5	[MnMoO$_3$(H$_2$L)(H$_2$O)$_2$]$_2$	3420sbr 3186s 3032s	1695vs 1664vs	1615vs 1594vs	1534s	—	1282m	1030w	940vs 909s 873s	540m 514m	—

turned blue. This further ruled out the possibility of the presence of ethanol molecules in the complexes. On the other hand, the essential feature of the band at ~3190 cm^{-1} in complexes (**3**) and (**5**) suggests that it most likely to arise from the stretching vibration of the secondary NH group of hydrazine.

The νC=O bands present at 1699 cm^{-1} and 1661 cm^{-1} in free dihydrazone are absent in all the heterobimetallic complexes except for complexes (**3**) and (**5**), which indicates the collapse of the amide structure of dihydrazone as a result of *enolization* on introduction of the second metal centre as a consequence of the heterometallic complex formation. The νC=O band present at 1669 cm^{-1} in the monometallic precursor [MoO$_2$(H$_2$L)]·H$_2$O complex shifts to higher frequencies on average by ~10 cm^{-1} and splits into two bands at ~1694 cm^{-1} and ~1665 cm^{-1}, similarly to that in uncoordinated dihydrazone in complexes (**3**) and (**5**) [15, 16]. Thus in complexes (**3**) and (**5**) the possibility of *enolization* of the >C=O group is ruled out and also the position of the νC=O band in complexes (**3**) and (**5**) dismisses the possibility of coordination of the >C=O group to the metal centres. The ν(C=N) band appears in these complexes as a couple of bands similar to those in free dihydrazone. This suggests that the two >C=N groups are not equivalent in the complexes. Such non-equivalency in >C=N groups indicates the coordination of dihydrazone to the metal centre in the *anti-cis* configuration, where the molecule is bent in such a manner that half hydrazone part is out-of-plane of the molecule and another half remains in the plane [49]. An interesting observation is that the ν(C=N) band shifts to higher frequencies by 1—3 cm^{-1} in all complexes except for complexes (**3**) and (**5**), in which this band shifts to lower frequencies by ca. 2 cm^{-1} as compared to that in the monometallic precursor complex. The shift

of the ν(C=N) band to higher frequencies in complexes (**1**), (**2**), and (**4**) indicates an increase in the >C=N bond order, whereas a lower shift indicates a decrease in the >C=N bond order in complexes (**3**) and (**5**). Such an increase in the bond order of the >C=N group in complexes (**1**), (**2**), and (**4**) indicates the flow of the electron density from the naphthyl ring to the metal centre through the azomethine nitrogen atom. This gives rise to a stronger azomethine nitrogen-to-metal bond, which may be related to the nature of the metal ion bonded to the azomethine nitrogen atom. The lowering in the >C=N bond order in complexes (**3**) and (**5**) is a result of a greater flow of the electron density from the azomethine nitrogen atom to the metal centre, giving rise to a stronger azomethine nitrogen-to-metal bond than that in the precursor complex. It is suggested that in all complexes, the parent metal ion, *i.e.,* the MoO_2^{2+} ion retains the N_2O_2 coordination sphere in all complexes, while in complexes (**3**) and (**5**) it is displaced by Ni^{2+} and Mn^{2+} from the N_2O_2 coordination sphere respectively. The Ni^{2+} and Mn^{2+} ions occupying the N_2O_2 coordination chamber draw greater electron density from the azomethine group than the MoO_2^{2+} group in the precursor monometallic complex. This assumption regarding the occupancy of the N_2O_2 coordination chamber by nickel and manganese ion rests entirely on the IR spectroscopic evidences and is purely tentative. This could not be confirmed by X-ray crystallographic studies because all our efforts to crystallize the compounds under different experimental conditions led to the precipitation of amorphous species.

Complex (**1**) shows a new band at 1510 cm^{-1} which is a characteristic of a newly created NCO^- group produced as a result of the *enolization* of dihydrazone [48, 49]. All the complexes show a strong to very strong band in the 1544—1531 cm^{-1} region. This band is assigned to have its origin in the ν(C—O)(naphtholate) vibration. The position of this band is consistent with the coordination of the naphtholate oxygen atom. However, in complexes (**1**), (**2**), and (**4**), the intensity is very high as compared to those in complexes (**3**) and (**5**). Hence, this band in complexes (**1**), (**2**), and (**4**), is suggested to have a contribution due to the stretching vibration of the NCO^- group produced as a result of the *enolization* of dihydrazone. The β(C—O) band appears in the 1292—1272 cm^{-1} region in the complexes. The ν(N—N) band appears in the 1095—1030 cm^{-1} region, similarly to that in the precursor monometallic complexes, indicating the coordination of only one hydrazinic nitrogen atom to the metal centre [51].

Heterobimetallic complexes Ni—MoO$_3$ (**3**) and Mn—MoO$_3$ (**5**) show three bands in the 968—873 cm^{-1} region, while heterobimetallic complexes Zn—MoO$_2$ (**1**), Cu—MoO$_2$ (**2**), and Co—MoO$_2$ (**4**) show only two bands in the 947—906 cm^{-1} region. The two bands present in the 947—904 cm^{-1} region in complexes (**1**), (**2**), and (**4**) are assigned to arise from the *cis*-MoO_2^{2+} unit [51]. However, in complexes (**3**) and (**5**), the three bands in the 968—873 cm^{-1} region are characteristic of the presence of the MoO$_3$ unit [52]. An unusual increase in the intensity of the band at 747 cm^{-1} in these complexes is attributed to arise due to a contribution of the ν_3(M$\langle^O_O\rangle$M) vibration band [53]. A new band observed at 875 cm^{-1} in complexes (**3**) and (**5**) indicates that it has originated from the tetra-atomic species M$\langle^O_O\rangle$M resulted from the involvement of the naphtholate oxygen atom in the bridge formation. The presence of this band indicates that nickel(II)/manganese(II) and molybdenum(VI) are held together through naphthoxo-bridging.

On examining the spectra of the ligand and the metal complexes below 600 cm^{-1}, the bands appearing in the 595—525 cm^{-1} and 474—433 cm^{-1} regions in complexes (**1**), (**2**), and (**4**) are tentatively assigned to ν(M—O)(naphtholic) and ν(M—O)(carbonyl) [15, 49, 54] respectively. The presence of new medium intensity bands at 554 cm^{-1}, 527 cm^{-1} and 540 cm^{-1}, 514 cm^{-1} in complexes (**3**) and (**5**) indicates that naphtholate oxygen atoms are bonded to the nickel and manganese atoms. On the other hand, the absence of bands at ~450 cm^{-1} in the complexes rules out the possibility of coordination of the carbonyl oxygen atom to the metal centre.

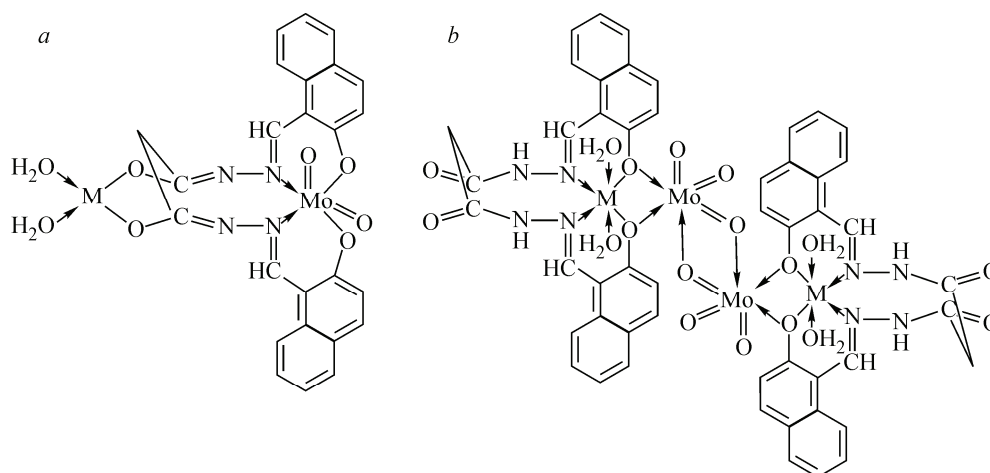*Fig. 3.* Tentative structures of the complexes: (*a*) [MMoO$_2$(L)(H$_2$O)$_2$] (M = Zn^{2+} (**1**), Cu^{2+} (**2**), Co^{2+} (**4**)) and (*b*) [{MMoO$_3$(H$_2$L)(H$_2$O)$_2$}$_2$] (M = Ni^{2+}(**3**), Mn^{2+} (**5**))

CONCLUSIONS

In the present study, five heterobimetallic complexes containing a molybdenyl ion as one component and some first row transition metal ions as another component from the monometallic precursor molybdenyl complexes [MoO$_2$(H$_2$L)]·H$_2$O of polyfunctional bis(2-hydroxy-1-naphthaldehyde)malonyldihydrazone have been isolated in the solid state and characterized. All complexes are non-electrolyte. Nickel and manganese heterometallic complexes are dimeric while the remaining complexes are monomeric. Dihydrazone is present in the *keto* as well as the *enol* form. Nickel(II) and manganese(II) ions displace the molybdenyl ion originally present in the NNOO coordination chamber while the remaining metal ions fail to do so and remain bonded to *enolate* oxygen atoms. MoO$_2^{2+}$, Ni(II), and Mn(II) ions have octahedral stereochemistry while Zn(II), Cu(II), and Co(II) have pseudotetrahedral stereochemistry in the heterobimetallic complexes.

The tentative structures of the complexes are given in Fig. 3.

REFERENCES

1. *Siegel A., Siegel H.* (Eds.) Metal Ions in Biological Systems (Molybdenum, Tungsten: Their Roles in Biological Processes), Vol. 39. – New York: Marcel Dekker, 2002.
2. *Gourlay C., Nielson D.J., White J.M., Knottenbelt Z., Kirk M.L., Young C.G.* // J. Amer. Chem. Soc. – 2006. – **128**, N 7. – P. 2164 – 2165.
3. *Majumdar A., Sarkar S.* // Coord. Chem. Rev. – 2011. – **255**, N 9-10. – P. 1039 – 1054.
4. *Dance I.* // Inorg. Chem. – 2011. – **50**, N 1. – P. 178 – 192.
5. *Liu C., Zhang H., Shi W., Lei A.* // Chem. Rev. – 2011. – **111**, N 3. – P. 1780 – 1824.
6. *Coelho A.C., Nolasco M., Balula S.S., Antunes M.M., Pereira C.C.L., Paz F.A.A., Valente A.A., Pillinger M., Ribeiro-Claro P., Klinowski J., Goncalves I.S.* // Inorg. Chem. – 2011. – **50**, N 2. – P. 525 – 538.
7. *Zhou W., Napoline J.W., Thomas C.M.* // Eur. J. Inorg. Chem. – 2011. – N 13. – P. 2029 – 2033.
8. *Li C., Cheng S., Tjahjono M., Schreyer M., Garland M.* // J. Amer. Chem. Soc. – 2010. – **132**, N 13. – P. 4589 – 4599.
9. *Miyazaki T., Tanabe Y., Yuki M., Miyake Y., Nishibayashi Y.* // Organometallics. – 2011. – **30**, N 8. – P. 2394 – 2404.
10. *Wheatley N., Kalck P.* // Chem. Rev. – 1999. – **99**, N 12. – P. 3379 – 3419.
11. *Jarenmark M., Haukka M., Demeshko S., Tuczek F., Zuppiroli L., Meyer F., Nordlander E.* // Inorg. Chem. – 2011. – **50**, N 9. – P. 3866 – 3887.
12. *Dutta S.K., Werner R., Flörke U., Mahanta S., Nanda K.K., Haase W., Nag K.* // Inorg. Chem. – 1996. – **35**, N 8. – P. 2292 – 2300.

13. *Rodríguez-Castellón E., Jiménez-López A., Eliche-Quesada D.* // Fuel. – 2007. – **87**, N 7. – P. 1195 – 1206.
14. *Wang D., Li X., Qian E.W., Ishihara A., Kabe T.* // Appl. Catal. A: Gen. – 2003. – **238**, N 1. – P. 109 – 117.
15. *Lal R.A., Chanu O.B., Borthakur R., Asthana M., Kumar A., De A.K.* // J. Coord. Chem. – 2011. – **64**, N 8. – P. 1393 – 1410.
16. *Kumar A., Borthakur R., Koch A., Chanu O.B., Choudhury S., Lemtur A., Lal R.A.* // J. Mol. Struct. – 2011. – **999**, N 1-3. – P. 89 – 97.
17. *Nath M., Saini P.K.* // Dalton Trans. – 2011. – **40**, N 27. – P. 7077 – 7121.
18. *Andruh M.* // Chem. Commun. – 2011. – **47**, N 11. – P. 3025 – 3042.
19. *Vigato P.A., Tamburini S., Bertolo L.* // Coord. Chem. Rev. – 2007. – **251**, N 11-12. – P. 1311 – 1492.
20. *Rajan O.A., Chakraborty A.* // Inorg. Chem. – 1981. – **20**, N 3. – P. 660 – 664.
21. *Vogel A.I.* A Text Book of Quantitative Inorganic Analysis. – London: Longman, 1973.
22. *Lintvedt R.L., Lynch W.E., Zehetmair J.K.* // Inorg. Chem. – 1990. – **29**, N 16. – P. 3009 – 3113.
23. *Carlson J.B., Davies G., Vouros P.* // Inorg. Chem. – 1994. – **33**. – P. 2334.
24. *Geary W.J.* // Coord. Chem. Rev. – 1971. – **7**, N 1. – P. 81 – 122.
25. *Nikolov A.V., Logvinenko V.A., Myachina L.I.* // Thermal Analysis, Vol. 2. – New York: Academic Press, 1969.
26. *Figgis B.N.* // Nature. – 1958. – **182**. – P. 1568 – 1970.
27. *Iskander M.F., El-Sayed L., Lasheen M.A.* // Inorg. Chim. Acta. – 1976. – **16**. – P. 147 – 157.
28. *Despaigne A.A.R., da Silva J.G., doCarmo A.C.M., Sives F., Piro O.E., Castellano E.E., Beraldo H.* // Polyhedron. – 2009. – **28**, N 17. – P. 3797 – 3803.
29. *Chan S.C., Koh L.L., Leung P.-H., Ranford J.D., Sim K.Y.* // Inorg. Chim. Acta. – 1995. – **236**, N 1-2. – P. 101 – 108.
30. *Kim B.-I., Miyake C., Imoto S.* // J. Inorg. Nucl. Chem. – 1975. – **37**, N 4. – P. 963 – 969.
31. *Kumar S.B., Chaudhury M.* // Dalton Trans. – 1991. – N 8. – P. 2169 – 2174.
32. *Bereman R.D., Shields G.D., Bordner J., Dorfman J.R.* // Inorg. Chem. – 1981. – **20**, N 7. – P. 2165 – 2169.
33. *Gullotti M., Casella L., Pintar A., Suardi E., Zanello P., Mangani S.* // Dalton Trans. – 1989. – N 10. – P. 1979 – 1786.
34. *Chang C.S.J., Collison D., Mabbs F.E., Enemark J.H.* // Inorg. Chem. – 1990. – **29**, N 12. – P. 2261 – 2267.
35. *Lever A.B.P.* // Coord. Chem. Rev. – 1968. – **3**, N 2. – P. 119 – 140.
36. *Lever A.B.P., Nelson S.M.* // J. Chem. Soc. A. – 1966. – N 7. – P. 859 – 863.
37. *Garloch M., Manning M.R.* // Inorg. Chem. – 1981. – **20**, N 4. – P. 1051 – 1056.
38. *Deeth R.J., Hitchman M.A., Lehman G., Sachs H.* // Inorg. Chem. – 1984. – **23**, N 10. – P. 1310 – 1320.
39. *Gewirth A.A., Cohen S.L., Schugar H.J., Solomon E.I.* // Inorg. Chem. – 1987. – **26**, N 7. – P. 1133 – 46.
40. *Hitchman M.A., Olson C.D., Belford R.L.* // J. Chem. Phys. – 1969. – **50**, N 3. – P. 1195 – 1203.
41. *van Dam P.J., Klaassen A.A.K., Reijerse E.J., Hagen W.R.* // J. Magn. Reson. – 1998. – **130**, N 1. – P. 140 – 144.
42. *Jiménez H.R., Salgado J., Moratal J.M., Morgenstern-Badarau I.* // Inorg. Chem. – 1996. – **35**, N 10. – P. 2737 – 2741.
43. *Pardi L.A., Hassan A.K., Hulsbergen F.B., Reedijk J., Spek A.L., Brunel L.C.* // Inorg. Chem. – 2000. – **39**, N 2. – P. 159 – 164.
44. *Li S., Hamrick Y.M., Van Zee R.J., Weltner W. Jr.* // J. Amer. Chem. Soc. – 1992. – **114**, N 11. – P. 4433 – 4434.
45. *Rubins R.S., Jani S.K.* // J. Chem. Phys. – 1977. – **66**, N 7. – P. 3297 – 3299.
46. *Barra A.L., Caneschi A., Gatteschi D., Sessoli R.* // J. Amer. Chem. Soc. – 1995. – **117**, N 34. – P. 8855 – 8856.
47. *Dowsing R.D., Gibson J.F., Goodgame D.M.L., Goodgame M., Hayward P.J.* // Nature. – 1968. – **219**. – P. 1037 – 1038.
48. *Degaonkar M.P., Puranik V.G., Tavale S.S., Gopinathan S., Gopinathan C.* // Bull. Chem. Soc. Jpn. – 1994. – **67**, N 7. – P. 1797 – 1801.
49. *Lal R.A., Chakrabarty M., Choudhury S., Ahmed A., Borthakur R., Kumar A.* // J. Coord. Chem. – 2010. – **63**, N 1. – P. 163 – 175.
50. *Braibanti A., Dallavalle F., Pellinghelli M.A., Leporati E.* // Inorg. Chem. – 1968. – **7**, N 7. – P. 1430 – 1433.
51. *Topich J., Bachert J.O. III* // Inorg. Chem. – 1992. – **31**, N 3. – P. 511 – 515.
52. *El-Hendawy A.M., Griffith W.P., Pumphrey C.A.* // J. Chem Soc. Dalton Trans. – 1988. – N 7. – P. 1817 – 1821.
53. *Percy G.C.* // J. Inorg. Nucl. Chem. – 1975. – **37**, N 10. – P. 2071 – 2073.
54. *Sacconi L., Sabatini A., Gans P.* // Inorg. Chem. – 1964. – **3**, N 12. – P. 1772 – 1774.